CERN - European Organization for Nuclear Research

LCD-Note-2013-006

Particle Identification with Cherenkov detectors in the 2011 CALICE Tungsten Analog Hadronic Calorimeter Test Beam at the CERN SPS

D. Dannheim*, K. Elsener*, W. Klempt*, A. Lucaci Timoce*, E. van der Kraaij†

* *CERN, Switzerland,* † *University of Bergen, Norway*

June 19, 2013

Abstract

In 2011 the CALICE Tungsten Analog Hadronic Calorimeter prototype (W-AHCAL) was exposed to mixed beams of electrons, pions, kaons and protons with momenta from 10 to 300 GeV in the CERN SPS H8 beam line. The selection of pion, kaon and proton samples is based on the information obtained from two Cherenkov threshold counters. This note presents the strategy for the particle identification, as well as the calibration, operation and analysis of the Cherenkov counters. Efficiency and sample-purity estimates are given for the data selected for the W-AHCAL data analysis.

1 Particle identification using Cherenkov threshold counters

Cherenkov threshold counters are used for the identification of relativistic charged particles. The Cherenkov detectors in the CERN test beams are implemented as several metre long cylindrical volumes with exchangeable gas (typically Helium, Nitrogen or CO_2) and pressure (typically between 20 mbar and 3 bar), installed in the beam lines upstream of the experimental areas. The created Cherenkov light is guided with a mirror to a photomultiplier and the amplified signal is discriminated with a fixed threshold and read out in coincidence with a scintillator particle counter, resulting in a binary information for each traversing particle. The probability to detect a signal depends on the operating conditions of the Cherenkov detector and on the particle type and momentum. The Cherenkov detectors can therefore be used to distinguish particles of different mass in a mixed beam.

1.1 Cherenkov light emission and diffractive index

Cherenkov light is emitted when a particle traverses an optical medium with a relativistic velocity $\beta = v/c$ higher than the speed of light in the medium c/n, where n is the index of refraction [1]. The Cherenkov light is emitted in a cone with an opening angle θ given by:

$$\cos(\theta) = 1/\beta n \approx 1 - \theta^2/2. \tag{1}$$

The relation $\beta^2 = 1 - m^2/p^2$ links the measurement of θ to the momentum and mass of the particle[1)]. The diffractive index n is tabulated for various gases at Standard Temperature and Pressure (STP: T=273 K and P_0=1 atm) [2]. Its dependence on pressure P and temperature T is given by the Lorentz-Lorenz formula, which for dilute gases can be approximated as:

$$n \approx \sqrt{1 + \frac{3AP}{RT}}, \tag{2}$$

where A is the molar refractivity and R is the universal gas constant.

The Cherenkov detectors used in test beams at CERN are usually operated with Helium, Nitrogen or CO_2. We obtain the corresponding diffractive indices n_{20} at the operation temperature of $T_{20} \approx 293$ K and for $P = 1$ atm using (2), see Table 1. Equation (2) yields in good approximation for the diffractive index $n(P)$ at $T = 293$ K and a given pressure P [atm]:

$$n(P) = 1 + P(n_{20} - 1). \tag{3}$$

1.2 Threshold pressure

The threshold pressure P_{th} above which Cherenkov light is observed is given for a charged particle with mass m and momentum p by equations (1) and (3). For $p \gg m$ we obtain for the limit case $\theta = 0$:

$$P_{th}[\text{atm}] = \frac{m^2}{2(1 - n_{20})p^2} \tag{4}$$

[1] Here and in the following we use natural units with c=1.

Table 1: Diffractive indices at $P = 1$ atm for gases frequently used in Cherenkov detectors.

gas	$n_0 - 1$ (T=273 K)	$n_{20} - 1$ (T=293 K)
He	3.50×10^{-5}	3.26×10^{-5}
N	2.98×10^{-4}	2.78×10^{-4}
CO_2	4.49×10^{-4}	4.18×10^{-4}

The pressure in bar (absolute) is related to the pressure in atm by the relation:

$$P[\text{atm}] = P[\text{bar}] * 1.01325. \tag{5}$$

Figure 1 shows the resulting threshold pressures in bar (absolute) for the two gases available in the CERN SPS test beams in 2011 (Nitrogen and Helium) and for different particle types at momenta between 0 and 300 GeV. Nitrogen results in a better separation between pions, kaons and protons[2)] for lower momenta ($p \lesssim 100$ GeV), while Helium extends the separation capability to larger momenta ($p \gtrsim 100$ GeV).

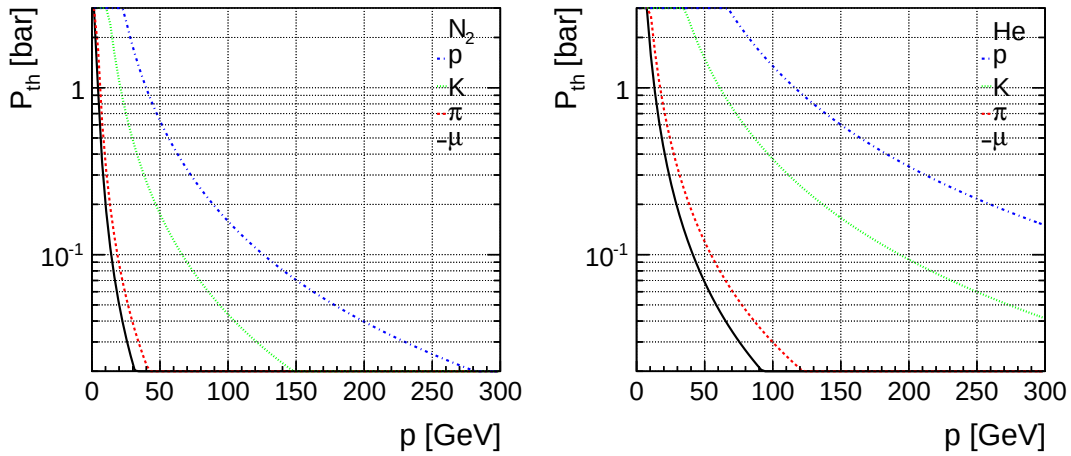

Figure 1: Calculated threshold pressures for the production of Cherenkov light from protons, kaons, pions and muons in Nitrogen (left) and Helium (right) at T=20°C. The range of the vertical axis corresponds to the operational range of the Cherenkov detectors installed in the SPS H8 beamline.

1.3 Cherenkov light intensity and detection efficiency

For small production angles θ, the average number of detected Cherenkov photoelectrons can be approximated as [3]:

$$N_{\text{pe}} = AL\theta^2, \tag{6}$$

[2]For simplicity, the term "proton" refers to both p and $\overline{p}$ in the following. Similarly, "pion" refers to both π^+ and π^- and "kaon" to both K^+ and K^-.

where L is the of the counter in cm and $A \lesssim 100$ is an empirical constant, depending on the wavelength of the Cherenkov light, the inefficiency of the optical system, the photon collection efficiency, the quantum efficiency of the photocathode and the discrimination threshold.

From equations 1, 4 and 6 we obtain for the average number of detected photo electrons:

$$N_{\text{pe}} = AL2(n-1)(P-P_{th}) \tag{7}$$

Assuming a Poissonian distribution for the number of detected photo electrons, the efficiency ε of the Cherenkov counter is given as the fraction of events for which at least one photo electron is observed:

$$\varepsilon = 1 - \exp(-N_{pe}) = 1 - \exp(-AL2(n-1)(P-P_{th})). \tag{8}$$

2 Particle content of the SPS H8 beams

The purity of the samples obtained with Cherenkov threshold counters depends on their efficiency and on the a-priori unknown particle content of the beam. A detailed Monte-Carlo simulation of the expected mixture of particles in the beam is beyond the scope of this analysis. Instead we discuss in the following the production and decay mechanisms for the simplified cases of production with a Beryllium target and in-flight decay in vacuum. The results of these analytical calculations are compared to the observed beam content in the W-AHCAL (muons) and in the Cherenkov detectors (pions, kaons and protons). Based on the estimated particle content and on the efficiencies of the Cherenkov counters for a given momentum and particle type (see section 3.2) we obtain the purity of the corresponding particle selection.

2.1 Beam conditions in the SPS H8 beam line

The observed particle content in the SPS H8 beam line depends on the production targets, the beam optics and the distance from the target. Figure 2 shows a sketch of the SPS H8 beam-line setup in 2011 with the approximate positions of the relevant beam-line instrumentations. For all runs considered here, the primary proton beam of 400 GeV was steared towards a Beryllium target approximately 605 m upstream the W-AHCAL. The resulting *secondary* beam was transported through a momentum selection and focusing system and an optional lead absorber. For some runs, a *tertiary* beam was created by inserting an additional copper target into the secondary beam. Further downstream are the two Cherenkov threshold counters "1" and "2" with a distance to the target of 464 m and 527 m, respectively. A system of two scintillator trigger detectors with an overlap area of approximately 10×10 cm^2 is located directly in front of the W-AHCAL prototype. The coincidence signal from the two scintillators is used to trigger the data aquisition of the W-AHCAL prototype. The information from the two Cherenkov threshold counters is only available for offline analysis.

A detailed description of the beam conditions for the dataset considered in the following can be found elsewhere [4]. Beams with negative or positive polarity and in a momentum range from 10 to 300 GeV were produced. Depending on the beam settings, the produced beams contained a mix of electrons, muons, pions, kaons and protons. In-flight decays of pions and kaons and interactions in collimators can significantly change the beam content along the path from the production to the two Cherenkov detectors and to the W-AHCAL.

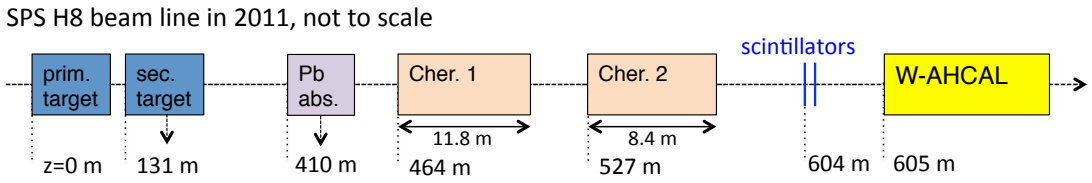

Figure 2: Schematic representation of the SPS H8 beam-line setup. The z axis corresponds to the direction of the beam and the approximate positions along z are given for the primary target, the optional secondary target, the optional lead absorber, the two Cherenkov threshold counters, the scintillators used for triggering and the W-AHCAL prototype, respectively.

2.2 Considered particle types

Electrons, muons, pions, kaons and protons are expected to be the main constituents of the produced beams. The respective contributions to the beam content can be estimated qualitatively with the following considerations.

2.2.1 Electrons/Positrons

A lead absorber with 18 mm thickness was used to efficiently remove electrons or positrons for the mixed hadron runs. In some early runs a different lead absorber configuration with only 8 mm thickness was used, leading to a small electron or positron contamination in the resulting hadron samples. This contamination can easily be removed by a selection based on the characteristic shower shapes resulting from purely electromagnetic interactions in the calorimeter, without using information from the Cherenkov detectors. Dedicated electron or positron runs were taken replacing the secondary copper target by a lead target and removing the absorber. These beam settings led to pure electron or positron samples, without the need for particle identification based on the Cherenkov detectors. Electrons and positrons are therefore not discussed any further in the following.

2.2.2 Muons

Muons are mainly created from in-flight decays of charged pions and kaons. Figure 3 shows the expected fraction of in-flight pion and kaon decays for initially pure pion and kaon beams in the H8 beam line as function of the beam momentum. The considered decay lengths correspond to the position of the two Cherenkov detectors and that of the W-AHCAL prototype and the distance between the first Cherenkov detector and the W-AHCAL prototype, respectively. For low momenta, the fraction of decays is large. At 50 GeV, 20% of all pions and 80% of all kaons decay before reaching the W-AHCAL surface. Pions decay with almost 100% branching ratio to muons and (anti-)neutrinos. Kaons decay with about 63% branching ratio to muons and (anti-)neutrinos. The remaining kaon decay channels are hadronic and semi-leptonic, leading to multi-particle pion and electron events that can be identified in the W-AHCAL analysis and are

thus not considered in the following. For the relevant momentum range from 10 to 300 GeV, the resulting opening angle between the muon and the initial pion or kaon direction is small, due to the large boost. The resulting muons, in particular the ones produced downstream of the large bending magnets, are therefore expected to be mostly contained in the acceptance of the W-AHCAL trigger system.

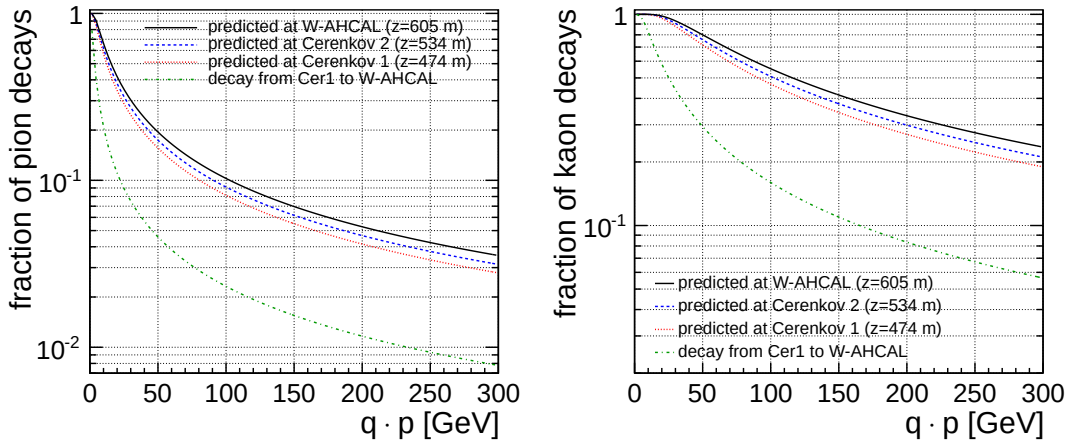

Figure 3: Expected fraction of in-flight decays in an intially pure beam of pions (left) and kaons (right). Shown are the predicted fraction of events in which the original particle has decayed, for different distances from the target, as well as the fraction of decays between the entrance of the first Cherenkov detector and the surface of the calorimeter.

While the in-flight decay contribution decreases with increasing beam momentum, additional muons can be produced at all energies in interactions along the beam line. The observed fraction of muon events in mixed hadron runs can therefore vary largely, depending on the collimator and beam-production settings. Pure dedicated muon beams were produced with thick absorbers (motorized beam dumps or closed collimators).

The identification of muons relies on the characteristic energy deposits of muon tracks in the W-AHCAL prototype. They can be selected or rejected with high efficiency based on the measurement of the total energy released in the W-AHCAL. Figure 4 (left) shows the observed distribution of the energy sum in the W-AHCAL for a tertiary hadron beam run with a momentum of 50 GeV and positive polarity. The unit MIPs refers to the energy deposit of minimum ionizing particles per calorimeter cell. The muon and hadron peaks can clearly be distinguished. The analysis of the mixed hadron runs presented in the following includes a rejection of muon events based on the total energy sum measured in the W-AHCAL prototype. Events are characterized as muons if the energy sum is between 45 and 150 MIPs. Events are considered as hadrons for energy sums above 150 MIPs. Figure 4 (right) shows the observed fraction of muon events based on this definition for all 2011 runs. Secondary and tertiary beams are distinguished with different marker styles. The observed muon fraction varies largely and no clear correlation with beam momentum or beam type (secondary / tertiary) is visible. The collimator settings are suspected to be the dominating cause of the varying muon content, as they were tuned for

each run to optimize the event rate in the W-AHCAL prototype. For all results presented in the following, only hadron-like events (with energy sum above 150 MIPs) are considered.

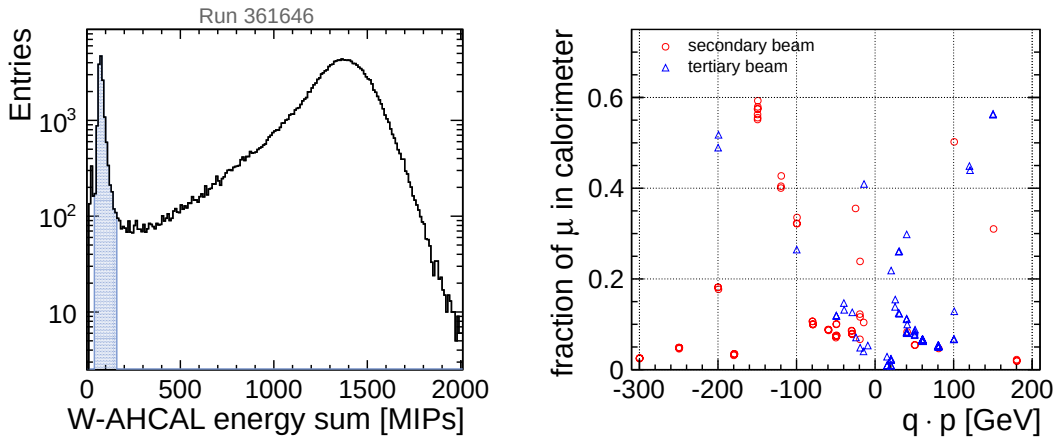

Figure 4: Distribution of the oberved energy sum in the calorimeter for a run at positive polarity and a momentum of $p_{beam} = 50$ GeV (left). The shaded area corresponds to the energy range used to select muons (45 MIPs$< \Sigma E <$ 150 MIPs) . The right plot shows the observed fraction of muons in the calorimeter for all runs and distinguishing between secondary and tertiary beams. Negative momentum values correspond to beams with negative polarity.

2.2.3 Pions, kaons and protons

Pions, kaons and protons are produced either in primary interactions of the 400 GeV proton beam with the Beryllium target or, for tertiary beams, in secondary interactions with the secondary copper target. Moreover, for certain beam conditions, hadron production within the collimator or absorber system may also contribute. For beams with negative polarity, pions are expected to be the largely dominating contribution, due to the large available phase space. Kaons on the other hand are expected to be suppressed due to strangeness conservation, both for negative and positive beam polarities. Similarly, the phase space for anti-proton production in beams with negative polarity is very small, leading to only a small expected fraction of anti-protons. On the other hand, the proton content is expected to be significant for positive beams at large momenta.

For the case of primary interactions of protons with a Beryllium target, a parametrization of a measurement of the corresponding flux of pions, kaons and protons for a given momentum and production angle is available [5, 6]. Figure 5 shows the resulting expected particle content for 400 GeV protons and 0 mrad production angle in the momentum range relevant for this analysis. The expected particle content at the W-AHCAL surface (z=605 m) is also shown, taking into account in-flight decays of pions and kaons, as described in section 2.2.2. An alternative presentation of the same parametrization is shown in Fig. 6, where the expected contributions from in-flight decays are removed from the samples, such that the normalization corresponds to

the fraction of all particles that do not decay before reaching the W-AHCAL. Within the limited validity of this model (secondary beam only, no further interactions of the produced particles), this allows for a comparison with the measured particle content of hadron beams, where muon events have been removed based on the energy sum observed in the W-AHCAL prototype.

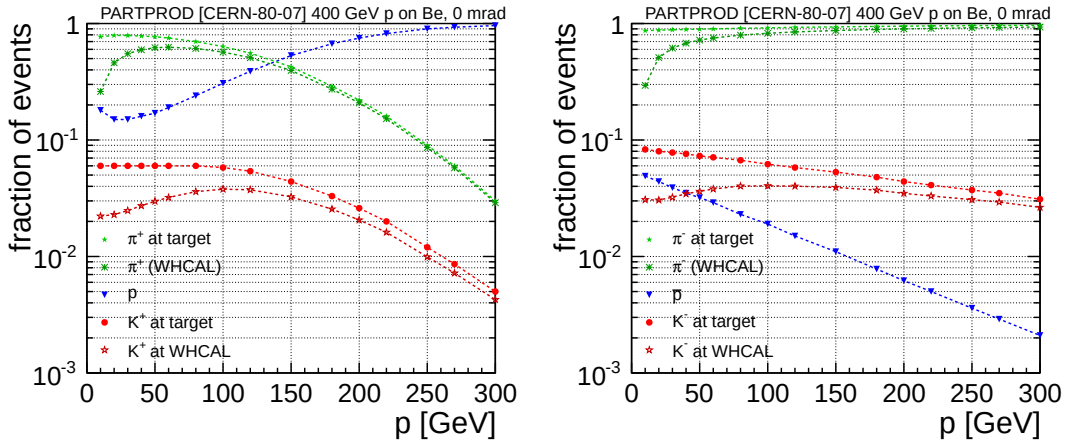

Figure 5: Expected particle content for secondary beams produced from collisions of 400 GeV protons with a Beryllium target at 0 mrad production angle [6]. The results are shown for positive (left) and negative (right) beam polarities. The expected particle content at the W-AHCAL surface (z=605 m) is also given, taking into account in-flight decays of pions and kaons.

3 Measurements of selection efficiencies and purities

3.1 Cherenkov detector operation

The two Cherenkov threshold-counters available in the SPS H8 beam line were used for particle identification in all 159 mixed hadron runs of the 2011 W-AHCAL data taking. While electrons and muons are efficiently identified based on calorimeter energy deposits (see section 2.2), the discrimination between pions, kaons and protons relies solely on the information provided by the Cherenkov detectors. The gas mixture and operation pressures were adjusted for each run. Detailed tables with the chosen gas mixture and pressure settings can be found elsewhere [4]. Figure 7 shows the chosen Cherenkov pressure settings for all runs as function of the beam momentum. Depending on the difference between the set pressure and the threshold pressure for a given particle type and momentum, one can obtain good selection efficiencies for all three considered particle types. Based on these one can obtain optimal selection criteria for a given run and particle type. The quality of this particle identification is determined by the efficiency and purity of the selection of a given particle type. The selection efficiencies of the two Cherenkov counters were determined from a dedicated set of calibration runs. The purity of the selection of a given (signal) particle type depends on the efficiency for selecting any other (background)

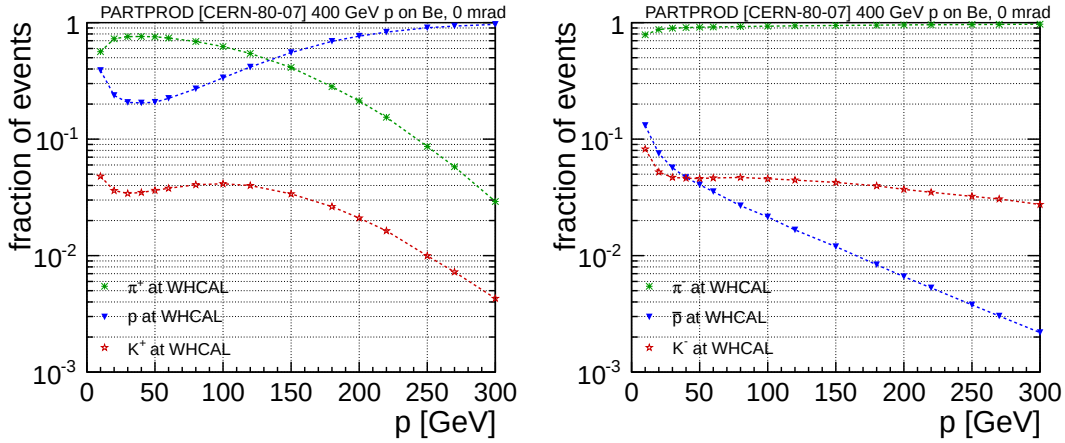

Figure 6: Expected particle content at the W-AHCAL surface (z=605 m) for secondary beams produced from collisions of 400 GeV protons with a Beryllium target at 0 mrad production angle [6]. The results are shown for positive (left) and negative (right) beam polarities. In-flight decays of pions and kaons are taken into account, but the normalization excludes all decay products.

particle type and on the particle content (number of signal and background particles in the beam). The particle content is estimated based on the considerations in section 2.2 and on an analysis of the observed event rates for various combinations of Cherenkov selections for each run.

3.2 Efficiency calibration

The turn-on characteristics (see section 1.3) of the two Cherenkov counters available in the SPS H8 beam line were measured in a dedicated set of runs at a negative-polarity beam of 50 GeV momentum and with pressures of Helium between 0.1 bar and 3 bar. For these runs the data-aquisition system of the W-AHCAL calorimeter prototype was disabled and events were counted over several beam spills requiring for each event a coincidence in the two scintillators mounted directly in front of the W-AHCAL surface. For each run the pressure in both counters was set to the same value and the number of events for three different categories was recorded:

- N(1): Number of events, in which Cherenkov counter 1 detected light in coincidence with the scintillator triggers.
- N(2): Number of events, in which Cherenkov counter 2 detected light in coincidence with the scintillator triggers.
- N(1&2): Number of events, in which both Cherenkov counters detected light in coincidence with the scintillator triggers.

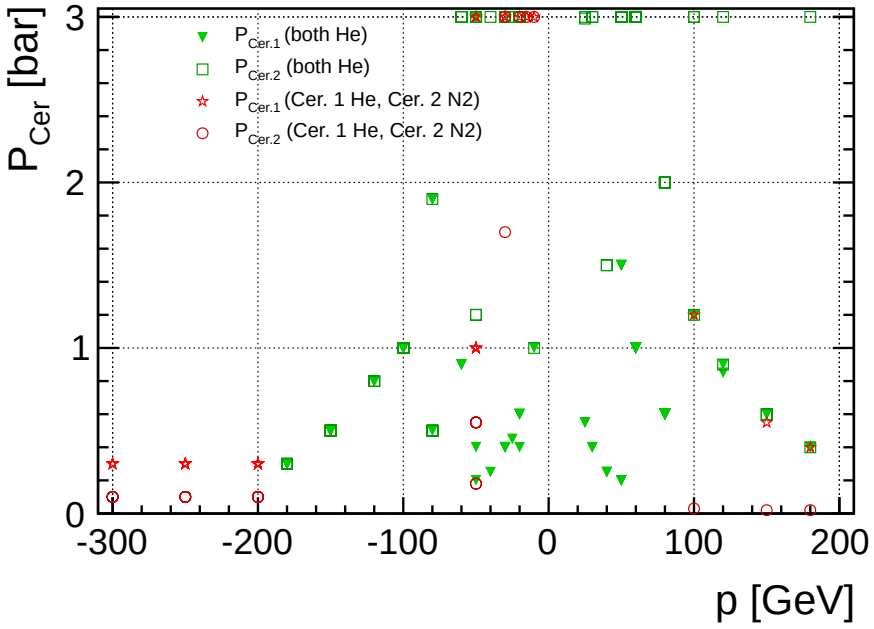

Figure 7: Pressure settings of the two Cherenkov detectors for all mixed hadron runs. The open markers correspond to runs where both Cherenkov detectors were filled with Helium. The filled markers correspond to runs where Cherenkov detector 1 was filled with Helium and Cherenkov detector 2 was filled with Nitrogen.

Assuming that the detection probabilities in both counters are independent, the efficiencies ε_1 and ε_2 of the two counters can be obtained with the tag-and-probe method:

$$\varepsilon_1 = \frac{N(1\&2)}{N(2)}\,, \qquad \varepsilon_2 = \frac{N(1\&2)}{N(1)} \tag{9}$$

The resulting efficiency turn-on curves are shown in Fig. 8 (left). The vertical error bars represent the statistical uncertainty of the counted event numbers. The horizontal error bars are fixed at 0.02 bar, corresponding to the assumed accuracy of the pressure settings. For 50 GeV momentum and negative beam polarity, pions are expected to be the dominating component of the beam (see section 2.2.3), with a threshold pressure of 0.12 bar. A fit of the parametrization (8) to the data points in the range 0.2 bar$\leq p \leq$ 3.0 bar is overlayed to the data points. The known length of the counters ($L_1 = 11.8$ m, $L_2 = 8.4$ m) is fixed in the fit and the quality factors $A_1 = 73.1$ and $A_2 = 77.7$ are obtained as the only free parameters of the fit. The large χ^2 value of 26 for the fit for the first counter indicates that the parametrization does not accurately describe the observed behaviour of the counter. The χ^2 value of 1.3 for the second counter indicates a better agreement between the data points and the parametrization within the fit range. (Note that the first data point at the threshold pressure of 0.1 bar is not included in the fits.) The observed efficiency value of approximately 7% for the second counter is not compatible with the expectation of 0% at threshold. The reason for the disagreement is not understood. It is however taken into account as a systematic uncertainty with an alternative parametrization of the efficiencies (see

below). A possible muon contamination of the beam was considered in a simultaneous fit to a muon ($p_{thr} = 0.07$ bar) and pion (p_{thr} =0.12 bar) component, leading however only to a small change in the resulting parametrization.

A linear interpolation between the measured data points is shown as solid lines in Fig. 8 (left). It results in a slightly smaller efficiency for most pressure values, compared to the fit. The linear interpolation is considered in the following as an alternative parametrization of the counter efficiencies. The difference between the results based on the fit and the ones from the linear interpolation is considered an estimate of the uncertainty originating from the Cerenkov counter calibration.

The quality factors A_1 and A_2 obtained with the 50 GeV pion calibration runs with Helium gas are used to obtain the corresponding efficiency parametrizations for the case of Nitrogen gas. In this case a linear interpolation between data points is not considered, as there was no dedicated set of calibration runs for Nitrogen performed. All parametrizations considered for the analysis presented in the following are shown in Fig. 8 (right) for the general case, i.e. as a function of the pressure above the threshold pressure.

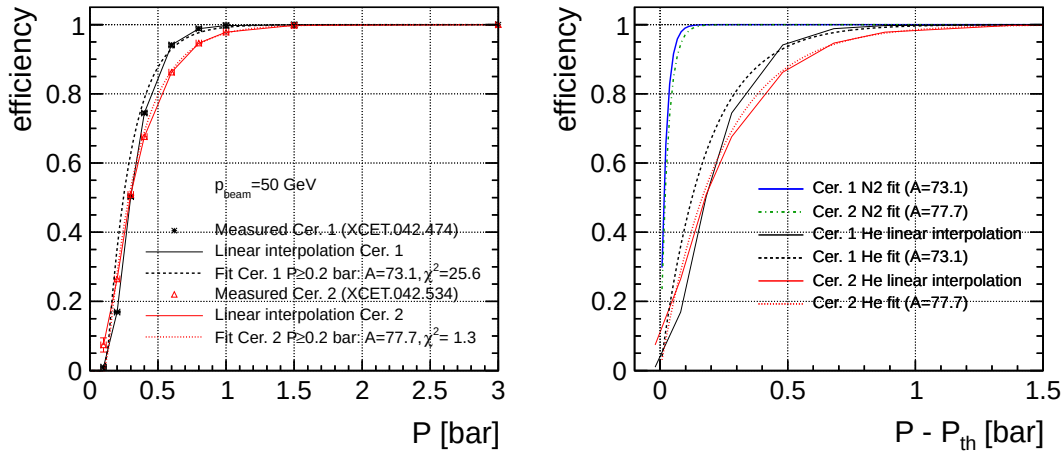

Figure 8: Efficiencies of the two Cherenkov threshold counters in the SPS H8 beam line, as obtained with the tag-and-probe method from a measurement with Helium at a beam momentum of $p_{beam} = 50$ GeV. The left plot shows the measured data points, a linear interpolation between them and the fit results for the parametrization as explained in the text. The right plot shows the parametrizations used in the analysis for both Nitrogen and Helium and as a function of pressure above the threshold pressure P_{th}.

3.3 Observed particle content

The particle content of each run is estimated based on an analysis of the observed event rates for the four disjunct samples selected by the corresponding response of the two Cherenkov detectors (Cer1 and Cer2): (1) Cer1 on & Cer2 off; (2) Cer1 off & Cer2 on; (3) Cer1 off & Cer2 off; (4) Cer1 on & Cer2 on. We assume that electrons and muons were efficiently removed from the

considered event samples using calorimeter information. For each selection, i, the number of observed events, $n_{\mathrm{obs},i}$ then depends on the number of pions, kaons and protons in the beam and on the corresponding selection efficiencies:

$$n_{\mathrm{obs},i} = \varepsilon_{\pi}^{i} \cdot n_{\pi} + \varepsilon_{K}^{i} \cdot n_{K} + \varepsilon_{p}^{i} \cdot n_{p} \tag{10}$$

The resulting over-constrained system of four linear equations with three unknowns is solved numerically using a singular-value decomposition (SVD) method, taking into account the statistical uncertainties of the observed event numbers [7]. Stable and meaningful solutions for n_{π}, n_{K} and n_{p} can only be expected in cases where the efficiencies for the different particle types differ significantly and sizeable event samples are observed for at least three out of the four disjunct selections.

Figure 9 shows the result of the SVD analysis for all 159 mixed hadron runs of the 2011 data taking period. The filled markers correspond to the case where the Cherenkov selection efficiencies are estimated from a fit to the calibration data, while the open markers correspond to a linear interpolation between the measured calibration data (see section 3.2). In most cases the efficiency estimates from the fit and from the linear interpolation result in very similar estimated event rates. For negative polarity runs with momenta above 30 GeV and for positive polarity runs with momenta above 80 GeV a separation between kaons and pions is not possible with the Cherenkov counter pressure settings chosen for the respective runs. The SVD analysis results have therefore been regularized by adding the event rates for kaons, which are expected to be very small, to the ones for pions (green markers). Similarly, for momenta below 50 GeV, a separation between kaons and protons is not possible. Here the expected event rates are of similar magnitude, leading to equal numbers for the estimated kaon and proton rates. The dashed lines in the plot show the PartProd expectations for secondary beams at 0 mrad production angle (see section 2.2.3). In general, a qualitative agreement between the observed pion event rates and the PartProd results can be seen. For runs with negative polarity, however, a larger anti-proton content of up to 10% is observed in the data, while the PartProd results predict only a very small anti-proton fraction that steeply falls with increasing momentum. Moreover, the expected drop in the pion content for low momenta, due to in-flight decays, is not observed in the data.

To investigate the influence of the beam conditions on the obtained event rates, a comparison between secondary and tertiary beams was performed. Figure 10 shows the results of the SVD analysis separately for secondary beams (open markers) and tertiary beams (filled markers). In both cases the results are obtained based on the fits to the measured Cherenkov efficiencies. No significant difference in the observed particle content between secondary and tertiary beams can be concluded.

3.4 Estimated selection purities and efficiencies

The purities $purity^{i}_{\pi,K,p}$ of the four disjunct Cherenkov selections ($i = 1...4$) introduced in section 3.3 can be otained for each run based on the respective efficiencies and estimated beam content:

$$purity^{i}_{\pi,K,p} = \frac{\varepsilon^{i}_{\pi,K,p} \cdot n_{\pi,K,p}}{\varepsilon^{i}_{\pi} \cdot n_{\pi} + \varepsilon^{i}_{K} \cdot n_{K} + \varepsilon^{i}_{p} \cdot n_{p}} \tag{11}$$

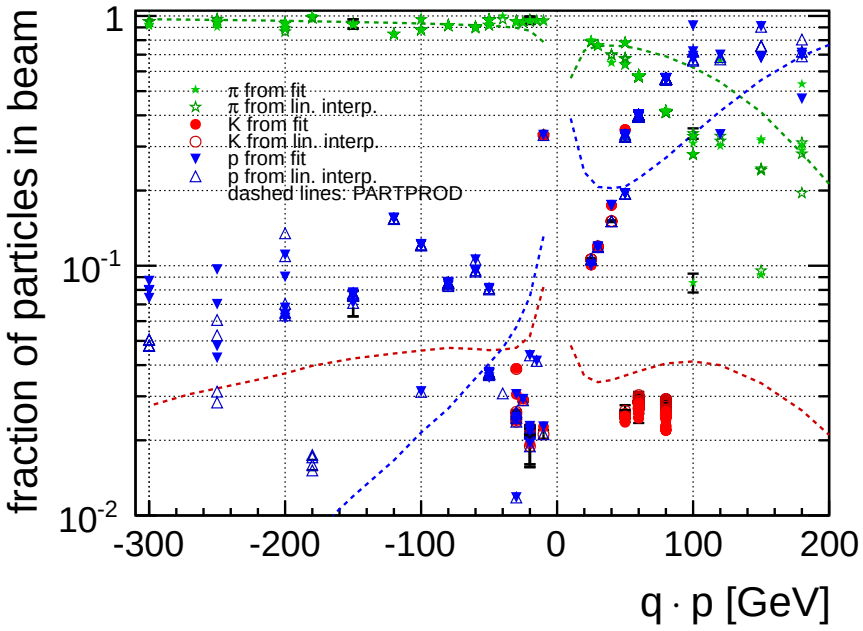

Figure 9: Observed particle content for all runs and for two different estimations of the Cherenkov selection efficiencies. The results are based on the observed event numbers for different Cherenkov threshold counter selections and using efficiency estimates from the fits and from the linear interpolation. The pion fraction for negative polarity runs with $p > 30$ GeV and for positive polarity runs with $p > 80$ GeV includes kaons. The dashed lines in the plot show the PartProd expectations for secondary beams at 0 mrad production angle.

The purity $purity_{\pi,K,p}$ for selecting a given particle type in a run is then defined as the maximum of the four purity values.

Figure 11 shows the resulting purities for all runs, based on the predicted beam content from PartProd and (a) on the efficiencies obtained with the fit method (filled markers) as well as (b) the ones obtained with the linear interpolation (open markers). For most runs the two different efficiency estimates lead to very similar purity results. In almost all runs a pure selection of pions ($> 90\%$) is achieved. Pure proton selections ($> 90\%$) are obtained for runs with a beam momentum of more than 40 GeV in runs with positive polarity. For lower momenta, the proton purity drops to approximately 85%. Anti-protons in negative polarity runs are pure ($> 90\%$) up to momenta of 120 GeV. Kaon selections with purities above 80% are obtained only in a few negative-polarity runs with momenta between 15 and 60 GeV and in positive polarity runs of 50 and 60 GeV.

To account for the increased anti-proton content obtained from the SVD analysis (see section 3.3), a separate analysis of the purities for the negative-polarity runs was performed. In this analysis the beam content was fixed to contain 90% pions, 3% kaons and 7% protons. The resulting purity estimates are shown in Fig. 12. The results are similar to the ones obtained based on the PartProd predictions, except that the proton selections for some of the low-momentum

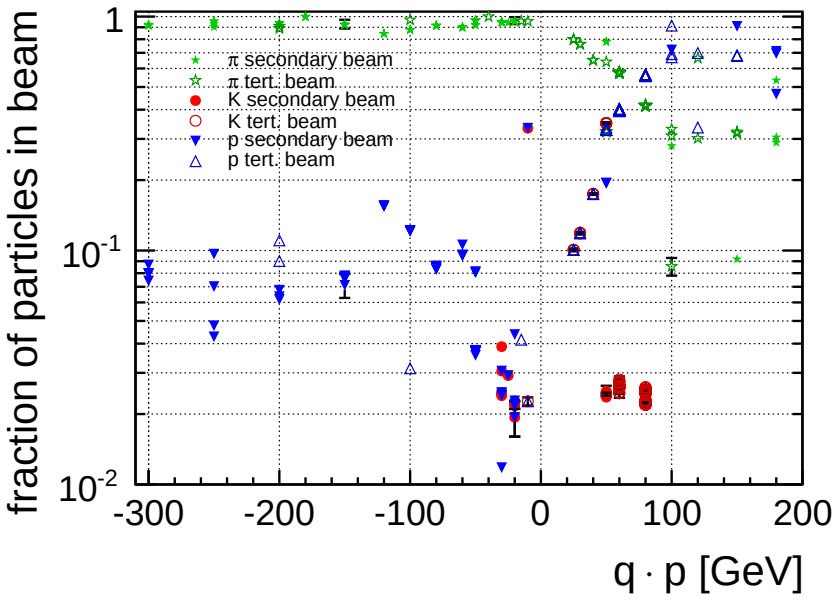

Figure 10: Observed particle content for all runs, distinguishing between runs with secondary (open markers) and tertiary (filled markers) beam settings. The results are based on the observed event numbers for different Cherenkov threshold counter selections and using efficiency estimates from the fits. The pion fraction for negative polarity runs with $p > 30$ GeV and for positive polarity runs with $p > 80$ GeV includes kaons.

runs show a reduced purity.

Figure 13 shows for all runs the efficiency of the respective pion, kaon and proton selection with highest purity. Figure 14 shows for all runs the achieved rejection power for the respective pion, kaon and proton selection with highest purities. The rejection power of a given selection is defined as the ratio between signal and background efficiency: $rejection = \varepsilon/(1 - purity)$.

Tables 2, 3 and 4 list all mixed hadron runs with pure selections ($> 80\%$) of pions, protons and kaons, respectively. The runs are grouped by beam momentum and the quoted purity and efficiency correspond to the respective average of the considered runs, weighted by the number of events in each run. The beam content predicted by PartProd is used to determine the purities. The event samples presented in these tables were used as input for the analysis of the W-AHCAL data [8]. The purity and efficiency shown in the table are based on the event selections used in the W-AHCAL analysis. In most cases they correspond to the ones with highest purity, as shown in Fig. 11 (right). In some cases sufficiently high purity was achieved with less restrictive selections, for example requiring only one of the two Cherenkov threshold counters to give a signal.

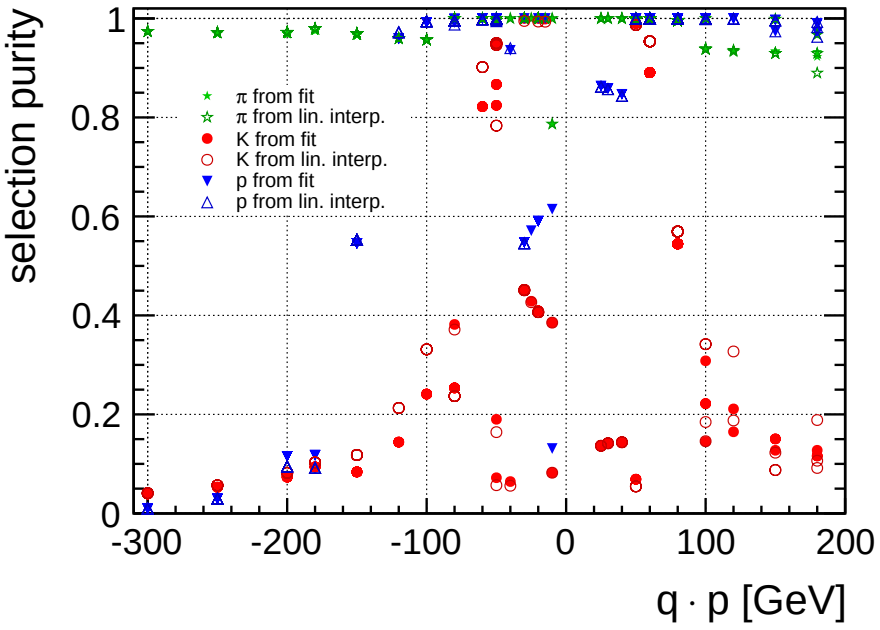

Figure 11: Estimated purities of the event selections corresponding to the highest purity for each run and particle type, based on the particle content predicted by PartProd.

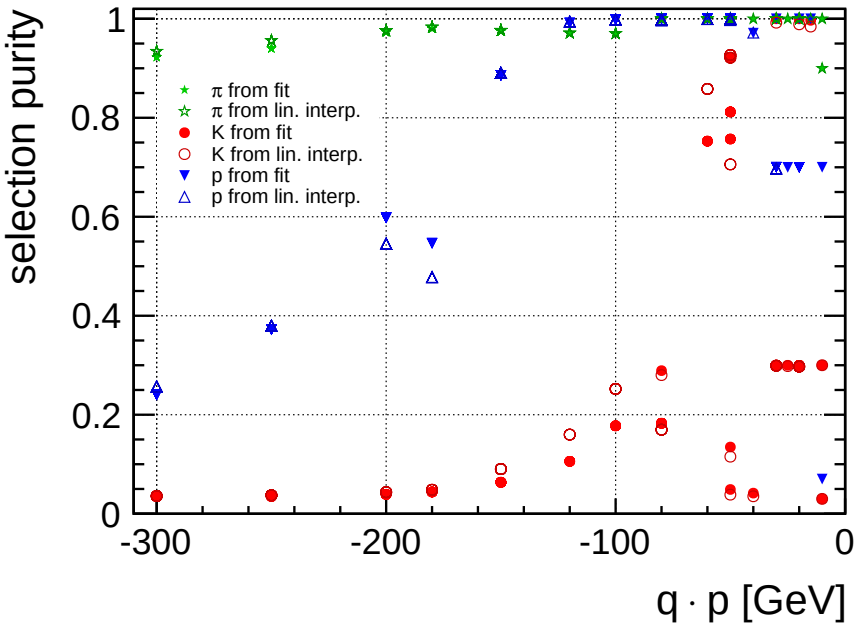

Figure 12: Estimated purities of the event selections corresponding to the highest purity for each run and particle type, based on an assumed fixed particle content of 90% pions, 3% kaons and 7% protons for all negative polarity runs.

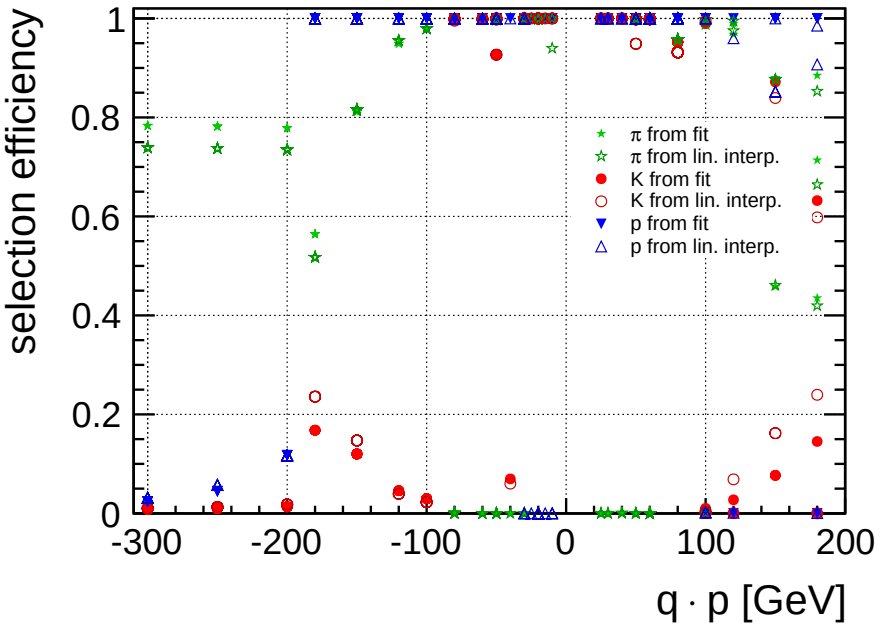

Figure 13: Efficiencies of the event selections corresponding to the highest purity for each run and particle type.

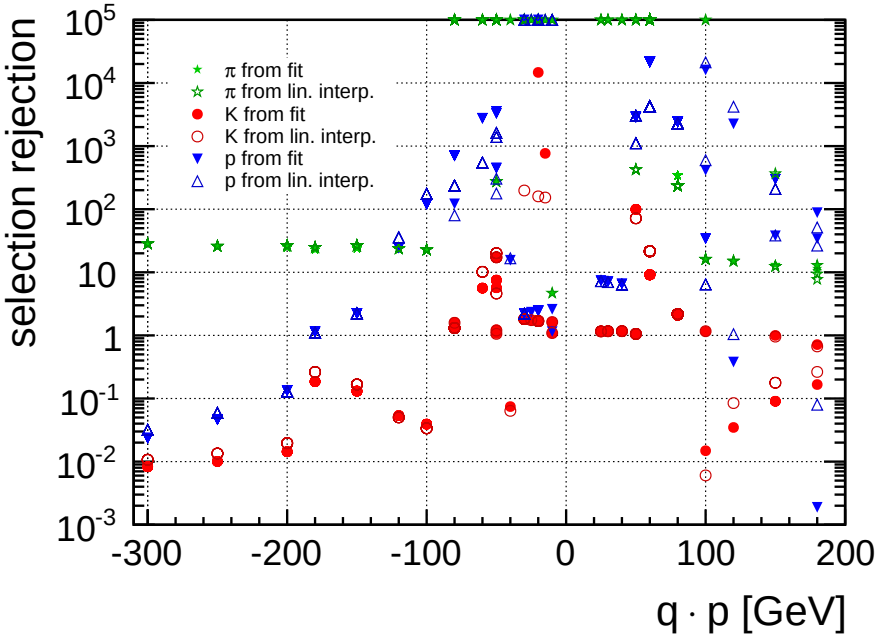

Figure 14: Rejection power of the event selections corresponding to the highest purity for each run and particle type. The rejection power is defined as $rejection = \varepsilon/(1 - purity)$ and is set to 10^5 for cases where the purity reaches 100%.

Table 2: Runs with pure ($> 80\%$) pion selection. The quoted purity and efficiency refer to the Cerenkov selections used in the W-AHCAL analysis and correspond to the average of all considered runs, weighted by the number of selected events in each run. Run numbers in bold correspond to runs with tertiary beam setttings.

q ·p [GeV]	# ev. sel.	purity	efficiency	run number - 361000
25	96514	100%	70%	**225 233**
30	151332	100%	70%	**216 217**
40	213184	100%	71%	**214 215**
50	383288	98%	88%	**235 249 250 646** 703 704
60	2014543	100%	99%	**645 659 660 661 664 665 666 667 668 669 670 671 672 673 681 683 719 720 721 722 724 726**
80	1501068	100%	95%	**728 729 730 731 732 733 735 737 738 739 740 741 756 757 758 759 760 761 762 763 765**
100	73466	95%	95%	621 **636 637 747**
120	64902	93%	98%	**643 745**
150	41529	93%	88%	619 **743 744**
180	56579	92%	87%	618 663 742
-10	26830	100%	100%	**471**
-15	105575	100%	100%	**470**
-20	526999	100%	100%	255 256 257 264 469
-25	140139	100%	100%	269
-30	748435	100%	84%	267 270 271 472 473
-40	133575	94%	71%	**253**
-50	1371469	99%	95%	273 274 375 415 479 480 481 482 483
-60	314198	100%	99%	354 356 357
-80	475632	100%	86%	351 376 377 400 416
-100	340177	96%	98%	**341** 352 353 404
-120	280329	96%	95%	358 359 405
-150	391386	97%	81%	360 361 406 407 408 409 410
-180	211185	98%	56%	369 371 372 412
-200	236246	97%	80%	427 428 431 **452 464**
-250	307326	96%	100%	426 434 436 448
-300	550201	97%	100%	424 425 450 451

Table 3: Runs with pure ($> 80\%$) proton selection. The quoted purity and efficiency refer to the Cerenkov selections used in the W-AHCAL analysis and correspond to the average of all considered runs, weighted by the number of selected events in each run. Run numbers in bold correspond to runs with tertiary beam setttings.

q $\times$p [GeV]	# ev. sel.	purity	efficiency	run number - 361000
25	33559	86%	100%	**225 233**
30	59383	86%	100%	**216 217**
40	106175	85%	100%	**214 215**
50	169775	100%	100%	**235 249 250 646** 703 704
60	1396605	100%	100%	**645 659 660 661 664 665 666 667 668 669 670 671 672 673 681 683 719 720 721 722 724 726**
80	2115700	100%	100%	**728 729 730 731 732 733 735 737 738 739 740 741 756 757 758 759 760 761 762 763 765**
100	205694	100%	100%	621 **636 637 747**
120	152651	99%	100%	**643 745**
150	233756	98%	100%	619 **743 744**
180	180429	96%	100%	618 663 742
-40	7085	94%	100%	**253**
-50	71759	100%	100%	273 274 375 415 479 480 481 482 483
-60	33985	100%	100%	354 356 357
-80	50770	100%	100%	351 376 377 400 416
-100	41815	99%	100%	**341** 352 353 404
-120	53288	96%	100%	358 359 405

Table 4: Runs with pure ($> 80\%$) kaon selection. The quoted purity and efficiency refer to the Cerenkov selections used in the W-AHCAL analysis and correspond to the average of all considered runs, weighted by the number of selected events in each run. Run numbers in bold correspond to runs with tertiary beam setttings.

q $\times$p [GeV]	# ev. sel.	purity	efficiency	run number - 361000
50	8765	99%	100%	358 359 405 **646** 703 704
60	105331	89%	100%	**645 659 660 661 664 665 666 667 668 669 670 671 672 673 681 683 719 720 721 722 724 726**
-15	141	100%	100%	**470**
-20	576	100%	100%	469
-30	6812	100%	100%	473
-50	18255	89%	98%	479 480 481 482 483
-60	1205	82%	100%	354 356 357

4 Summary and conclusions

Two Cherenkov counters installed in the SPS H8 beam line were used for the identification of pions, kaons and protons in the W-AHCAL runs. The beam composition was estimated based on the observed event yields. Results obtained with the particle production-rate calculator PartProd served as an additional rough estimate of the beam composition.

The efficiencies and purities of the event selection are limited by the operating constraints of the Cherenkov counters. Moreover the determination of the selection purities is hampered by large fluctuations in the beam conditions and by the fact that the beam composition is a-priory not known. Further systematic limitations for the accuracy of the presented measurements are the accuracy and consistency of the Cherenkov counter calibration.

Despite these limitations, operating the Cherenkov counters sufficiently far from the respective thresholds resulted in pure pion, kaon and proton samples in a sizeable fraction of the runs recorded at the SPS in 2011. These samples are used in the W-AHCAL data analysis described in detail in [8].

References

[1] J. D. Jackson. *Classical Electrodynamics, Third Edition*. Wiley, New York, 1999.

[2] Particle Data Group. Atomic and Nuclear Properties of Materials (online compilation). http://pdg.lbl.gov/2012/AtomicNuclearProperties/, 2012.

[3] J. Litt and R. Meunier. Cerenkov counter technique in high-energy physics. *Annu. Rev. Nucl. Sci.*, vol. 23 pp. 1–43. 43 p, 1973.

[4] D. Dannheim, W. Klempt and E. van der Kraaij. Beam tests with the CALICE tungsten analog hadronic calorimeter prototype. LCD-Note-2012-002, 2012.

[5] H. W. Atherton, et al. *Precise measurements of particle production by 400 GeV/c protons on beryllium targets*. CERN-80-07, Geneva, 1980.

[6] PartProd online calculator for particle production rates in interactions of protons with a Beryllium target. Website: `http://gatignon.home.cern.ch/gatignon/partprod.html`.

[7] Singular Value Decomposition (SVD) algorithm, implemented in ROOT. Website: `http://root.cern.ch/root/html/TDecompSVD.html`.

[8] A. Lucaci-Timoce. Status report on the analysis of the 2011 CALICE W-AHCAL data. LCD-Note-2013-002 in preparation, 2013.